

University of Groningen

Targeted imaging of integrins in cancer tissues using photocleavable Ru(ii) polypyridine complexes as mass-tags

Han, Jiaying; Sun, Jing; Song, Shanshan; Beljaars, Leonie; Groothuis, Geny M M; Permentier, Hjalmar; Bischoff, Rainer; Halmos, Gyorgy B; Verhoeven, Cornelia J; Amstalden van Hove, Erika R

Published in:
Chemical communications (Cambridge, England)

DOI:
[10.1039/d0cc00774a](https://doi.org/10.1039/d0cc00774a)

IMPORTANT NOTE: You are advised to consult the publisher's version (publisher's PDF) if you wish to cite from it. Please check the document version below.

Document Version
Publisher's PDF, also known as Version of record

Publication date:
2020

[Link to publication in University of Groningen/UMCG research database](#)

Citation for published version (APA):

Han, J., Sun, J., Song, S., Beljaars, L., Groothuis, G. M. M., Permentier, H., Bischoff, R., Halmos, G. B., Verhoeven, C. J., Amstalden van Hove, E. R., Horvatovich, P., & Casini, A. (2020). Targeted imaging of integrins in cancer tissues using photocleavable Ru(ii) polypyridine complexes as mass-tags. *Chemical communications (Cambridge, England)*, 56(44), 5941-5944. <https://doi.org/10.1039/d0cc00774a>

Copyright

Other than for strictly personal use, it is not permitted to download or to forward/distribute the text or part of it without the consent of the author(s) and/or copyright holder(s), unless the work is under an open content license (like Creative Commons).

The publication may also be distributed here under the terms of Article 25fa of the Dutch Copyright Act, indicated by the "Taverne" license. More information can be found on the University of Groningen website: <https://www.rug.nl/library/open-access/self-archiving-pure/taverne-amendment>.

Take-down policy

If you believe that this document breaches copyright please contact us providing details, and we will remove access to the work immediately and investigate your claim.



Cite this: *Chem. Commun.*, 2020, 56, 5941

Received 30th January 2020,
 Accepted 21st April 2020

DOI: 10.1039/d0cc00774a

rsc.li/chemcomm

Targeted imaging of integrins in cancer tissues using photocleavable Ru(II) polypyridine complexes as mass-tags†

Jiaying Han,^a Jing Sun,^b Shanshan Song,^a Leonie Beljaars,^a Geny M. M. Groothuis,^a Hjalmar Permentier,^a Rainer Bischoff,^{id} Gyorgy B. Halmos,^{id} Cornelia J. Verhoeven,^{id} Erika R. Amstalden van Hove,^{de} Peter Horvatovich^{id}*^{af} and Angela Casini^{id}*^{af}

Targeted epitope-based mass spectrometry imaging (MSI) utilizes laser cleavable mass-tags bound to targeting moieties for detecting proteins in tissue sections. Our work constitutes the first proof-of-concept of a novel laser desorption ionization (LDI)-MSI strategy using photocleavable Ru(II) polypyridine complexes as mass-tags for imaging of integrins $\alpha v \beta 3$ in human cancer tissues.

Imaging the distribution of specific proteins in tissues can provide new insights into biological processes related to the functioning of cells, the molecular mechanisms of diseases and drug action, and can also be used for diagnosis. Amongst the possible investigational methods, mass spectrometry imaging (MSI) constitutes a powerful and versatile technique for the multiplexed analysis of a broad variety of molecules ranging from metabolites (metabolomics), proteins (proteomics), metal ions (metallomics) and pharmaceutical compounds.^{1–4} A powerful technique in mass spectrometry for tissue section analysis is matrix-assisted laser desorption ionization-mass spectrometry imaging (MALDI-MSI),^{5–8} providing information about both the simultaneous spatial distribution and relative abundance of hundreds of unknown compounds within tissue sections.⁹ To date, significant innovations, especially in instrumentation¹⁰ and sample preparation protocols, have allowed analysis of both fresh, frozen and formalin-fixed paraffin-embedded (FFPE) tissues

by MALDI-MSI.¹¹ However, the application of this powerful method is still restricted by several limitations stemming from the nature of tissue samples, as well as from the MALDI-MSI process.¹² One of the main issues is the requirement of a matrix and its preparation and deposition procedure, limiting the ionization efficiency, reproducibility, spatial resolution, and the detection of low abundant proteins, as well as the size of the molecules detectable by the MALDI process.¹³

To achieve specific or targeted protein detection in tissue by MSI, especially in FFPE tissues, an affinity-based strategy involving the use of ‘mass-tags’ has been developed, wherein a probe is directed against a specific molecular target. The probe features a reporter group, namely a mass-tag, which is an encoding molecule with a specific mass, released as a cation from the tissue during the MALDI process. Usually, mass-tags are small molecules (< 1000 Da) with high ionization efficiency. Upon laser irradiation, the mass-tag is cleaved from the targeting molecule on the tissue surface, ionized and detected by mass spectrometry, thus, providing indirect target identification with localization information.^{14,15} Depending on the photocleavage efficiency, the method can be performed also under matrix-free laser desorption ionization (LDI) conditions.

Olejnik and coworkers developed the first photocleavable (PC) mass-tags for targeted detection of proteins in 1998,¹⁶ whereby a specific antibody was tethered to a mass-tag through a PC-linker, namely a 2-nitrobenzyl derivative. In 2007, Fournier and coworkers¹⁵ reported mass-tag approaches for targeted MALDI-MSI of proteins and mRNA in tissues with 4-[4-[1-(Fmoc-amino)ethyl]-2-methoxy-5-nitrophenoxy]butanoic acid as PC-linker. The mass-tag strategy was extended to different types of affinity binders including antibodies, lectins or aptamers.¹⁷ Gut and coworkers¹⁴ developed matrix-free TAMSIM (TARgeted multiplex Mass Spectrometry IMaging) using trityl (triaryl methane) species as mass-tags, forming resonance stabilized carbocations upon laser irradiation. In 2012, Caprioli and coworkers¹⁸ developed an activity-based MSI approach using reporter trityl mass tags, providing high spatial resolution and sensitivity through the combination of signal amplification chemistry and target specificity.

^a Groningen Research Institute of Pharmacy, University of Groningen, Antonius Deusinglaan 1, 9713 AV Groningen, The Netherlands.
 E-mail: p.lhorvatovich@rug.nl

^b Zernike Institute for Advanced Materials, University of Groningen, The Netherlands

^c Department of Otorhinolaryngology/Head and Neck Surgery, University Medical Center Groningen, University of Groningen, The Netherlands

^d Division of BioAnalytical Chemistry, Amsterdam Institute for Molecules Medicines and Systems, Free University of Amsterdam, The Netherlands

^e ERA Advanced Analytics, Amsterdam, The Netherlands

^f Chair of Medicinal and Bioinorganic Chemistry, Department of Chemistry, Technical University of Munich, Lichtenbergstr. 4, 85748 Garching, Germany.
 E-mail: angela.casini@tum.de

† Electronic supplementary information (ESI) available. See DOI: 10.1039/d0cc00774a

Overall, photocleavable mass-tag strategies have been successfully implemented in the field of targeted imaging of proteins, which can be applied independently from the protein mass and ionization affinity.^{19,20} Moreover, this approach can be combined with hybridization and affinity recognition techniques including *in situ* hybridization of mRNA (ISH) and immunohistochemistry (IHC). Despite these promising results, drawbacks of the mass-tags developed to date include: (i) the preparation of the tags often requires sophisticated and elaborate synthesis and purification steps of the linker-reporter moiety, (ii) stability issues of the tag itself (as in the case of TAMSIM¹⁴), (iii) lack of specific mass spectral features such as the isotopic pattern to facilitate data processing and compound identification.

In order to overcome the above-mentioned limitations, our group developed a mass-tag constituted of a photocleavable Ru(II) polypyridine complex tethered to a targeting peptide. Upon photoexcitation, ruthenium polypyridyl compounds are known to selectively photosubstitute one ligand of the coordination sphere by a solvent molecule.^{21–23} Therefore, upon UV light activation inside the mass spectrometer ionization chamber, a ruthenium-containing charged fragment is released from the tagged peptidic moiety, providing a fingerprint signal in the MS spectrum. Not only is the ionization efficiency of the photocleaved positively charged Ru(II) fragment high, but the metal ion also has a specific isotopic pattern distribution which renders its identification unambiguous. Moreover, it was hypothesized that this approach would enable matrix-free MSI. The absence of a matrix simplifies the preparation of the tissue and facilitates improvement of the MSI reproducibility, avoiding the interferences due to the matrix crystallization process.

Following this approach, a PC Ru(II) polypyridyl complex was bioconjugated to the cyclic cyc(RGDfK) peptide which specifically binds to integrins $\alpha v \beta 3$.^{24,25} The expression of the latter has been shown to correlate well with metastasis and tumor neovascularization.^{26–29} In our study, the Ru(II) mass-tag was used to image $\alpha v \beta 3$ integrins in samples of hypopharynx tumor tissue from a human patient with head and neck cancer. In this type of cancer, $\alpha v \beta 3$ integrins are not necessarily overexpressed with respect to normal cells, but they have a characteristic tumor tissue distribution as shown by previous IHC studies.³⁰

Initially, an already reported synthetic route was used to prepare the $[\text{Ru}^{\text{II}}(\text{terpy})(\text{bpy})\text{Cl}]^+$ complex (**1**,^{31,32} Scheme 1) (see Experimental section for details and Fig. S1, ESI[†]). Afterwards, the compound

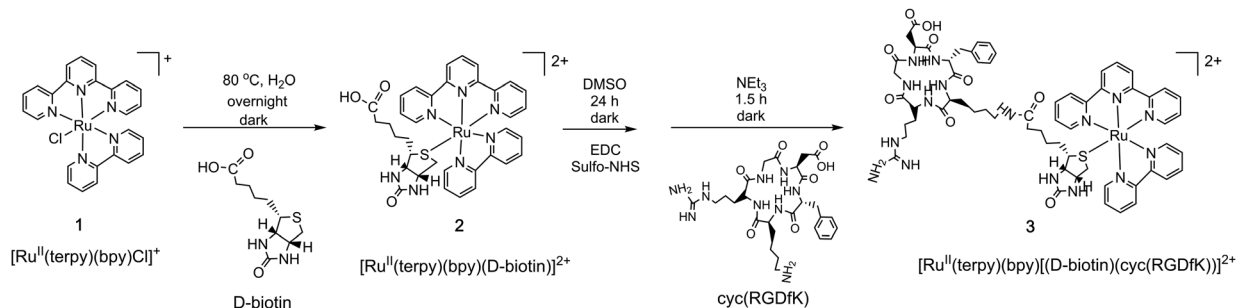
was derivatized with biotin *via* exchange of the chlorido ligand with a thioether group, with high affinity for Ru(II), following a previously reported procedure.³³ The Ru–biotin complex $[\text{Ru}^{\text{II}}(\text{terpy})(\text{bpy})(\text{D-biotin})]^{2+}$ (**2**, Scheme 1 and Fig. S2, ESI[†]) could then be further tethered to the targeting peptide by amide bond formation, through the carboxylic moiety present on the biotin ligand.

The synthesis of the bioconjugated targeted mass-tag $[\text{Ru}^{\text{II}}(\text{terpy})(\text{bpy})(\text{D-biotin})(\text{cyc}(\text{RGDfK}))]^{2+}$ (**3**) was achieved by directly conjugating **2** to the cyc(RGDfK) peptide by first activating the Ru(II) compound *via* EDC (1-ethyl-3-(3-dimethylamino-propyl)carbodiimide) and sulfo-NHS (*N*-hydroxysulfosuccinimide) treatment, followed by addition of 1.1 equiv. of peptide for 1.5 h at room temperature in the dark. Compound **3** was purified on a C18 column and analyzed by HPLC-MS (see Experimental for details and Fig. S3, ESI[†]). The UV-visible absorption spectrum of compound **3** showed two typical bands at 315 nm and 450 nm (Fig. S4, ESI[†]).

To investigate the feasibility of matrix-free LDI-MSI, the photocleavable character of compound **3** ($2 \mu\text{g mL}^{-1}$) was assessed by LDI-MS without matrix, with the compound deposited on an ITO coated glass slide. Ruthenium species due to photocleavage of the Ru mass-tag **3** upon UV laser irradiation are clearly detected (Fig. S5, ESI[†]). A main monocharged species appears at m/z 567.087, which was attributed to a $[\text{Ru}^{\text{II}}(\text{terpy})(\text{bipy})(\text{pyridine})\text{-3H}]^+$ fragment. The latter is not unexpected since previous mass spectrometry studies, including LDI and MALDI MS, on similar Ru(II) polypyridine complexes have shown that a bipyridine ligand may also fragment, releasing a pyridine ring which can further react with the ruthenium centre.^{34–36} As a result of this fragmentation, other Ru(II)-pyridine species are detected in the mass spectrum (Fig. S5, ESI[†]). Moreover, fragmentation of the terpy ligand has been excluded based on the in depth analysis of the MS data and on previously reported MS studies on similar complexes.³⁷

The affinity of the Ru(II) mass-tag **3** for its target $\alpha v \beta 3$ integrins ($\text{IC}_{50} = 3.2 \pm 0.5 \text{ nM}$) was validated by an ELISA-type solid-phase binding assay.^{25,38,39} The results also showed that **3** has much lower binding affinity for integrins $\alpha_5 \beta_1$ and $\alpha_v \beta_5$ (IC_{50} ca. 500 nM), indicating its selectivity.

The expression and distribution of integrin $\alpha v \beta 3$ in tumor samples was confirmed in tissue sections collected from patients with hypopharyngeal squamous cell carcinoma using IHC and hematoxylin staining. The results showed integrins



Scheme 1 Synthesis of the Ru(II) mass-tag compound **3**, $[\text{Ru}^{\text{II}}(\text{terpy})(\text{bpy})(\text{D-biotin})(\text{cyc}(\text{RGDfK}))]^{2+}$.

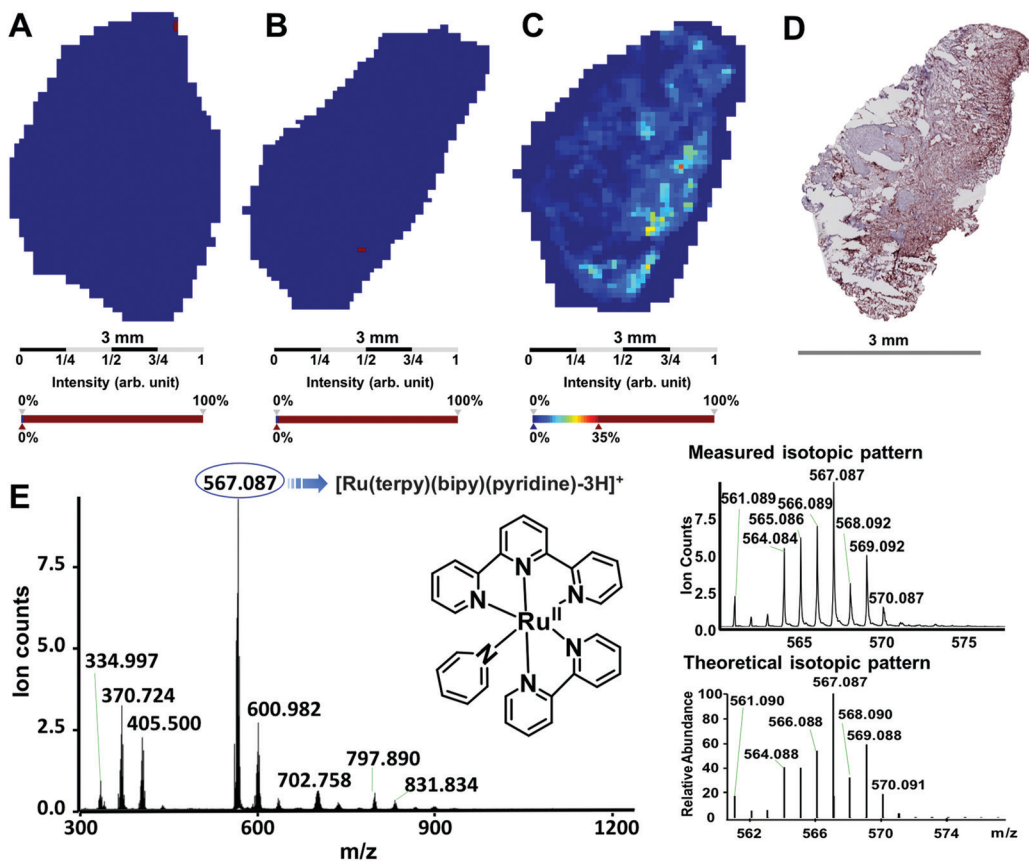


Fig. 1 LDI-MSI images of mass-tag from hypopharynx tumor tissue sections incubated with (A) PBS buffer (pH 7.4), (B) compound **2** $[\text{Ru}^{\text{II}}(\text{terpy})(\text{bpy})\text{-}(\text{D-biotin})]^{2+}$ and (C) compound **3** $[\text{Ru}^{\text{II}}(\text{terpy})(\text{bpy})(\text{D-biotin})(\text{cyc}(\text{RGDfK}))]^{2+}$. Images were obtained with a m/z range of 560.43–571.91 Da, which covers all isotopes of the Ru mass tags in the LDI spectrum. (D) $\alpha v \beta 3$ IHC and haematoxylin stained section of a hypopharyngeal squamous cell carcinoma section. The dark red staining represents the localization of the target integrin. (E) LDI mass spectrum of the mass-tag signal related to the image of sections incubated with compound **3** (pixel coordinates: x 25, y 34, pixel ID 131). The inset shows the experimental isotopic pattern distribution of the main fragment ion $[\text{Ru}(\text{terpy})(\text{bipy})(\text{pyridine})\text{-}3\text{H}]^+$ vs. the theoretical one (mass range from m/z 560 to 575). Images A, B and C were obtained with the “weak denoising” option of the SCiLS software. The images without denoising can be found in the ESI † (Fig. S7) as well as magnified areas of slices C and D (Fig. S8).

$\alpha v \beta 3$ were highly expressed (crimson color) in the tumor stroma (Fig. S6, ESI †) in line with previous results.³⁰ LDI-MSI experiments were performed on three tissue sections incubated with PBS buffer (pH 7.4), compound **2** or compound **3**, respectively (Fig. 1). The results were compared with IHC and hematoxylin staining performed on adjacent tissue sections. The significantly higher intensities of LDI signals in the sections treated with compound **3** compared to the two other tissue sections was confirmed in the intensity distribution diagrams of MS peaks in the whole MSI dataset (ESI † , Fig. S7).

Incubating the tissue section with compound **3** resulted in a clearly distinguishable signal corresponding to the distribution of the mass-tag (Fig. 1C). It should be noted that the high intensity signal of the Ru(II) polypyridine mass-tag (Fig. 1E), features the same isotope pattern as the one from compound **3** ($2 \mu\text{g mL}^{-1}$) deposited on the ITO coated glass slide (Fig. S1, ESI †). In the tissue, the distribution of the signal arising from complex **3** correlates well with the distribution of $\alpha v \beta 3$ integrins based on IHC and hematoxylin staining (Fig. 1D and Fig. S8, ESI †), while the LDI-MSI images of the control with PBS (Fig. 1A) show no signal in the m/z range of the mass-tag.

Concerning tissue treated with compound **2** (Fig. 1B), unspecific and scarcely intense Ru signals were detected due to residual presence of the compound following the washing steps. These results demonstrate that only the integrin targeted construct **3** results in the expected distribution of the mass-tag in the tissue section, while compound **2**, with only D-biotin as ligand, does not bind to any specific region of the section.

In this proof-of-concept study, we propose a matrix-free LDI-MSI strategy using a novel metal-based photocleavable mass-tag targeted at integrin receptors, namely the ruthenium complex **3** $[\text{Ru}^{\text{II}}[(\text{terpy})(\text{bpy})(\text{D-biotin})(\text{cyc}(\text{RGDfK}))]^{2+}$. The mass-tag of the Ru(II) polypyridine moiety provides a specific isotopic pattern, enabling differentiation of the tag from background signals. Ideally this strategy may be extended to reveal the spatial distribution of other proteins in tissue samples without limitation of the mass range of the target analytes by conjugating Ru(II) polypyridyl fragments $[\text{Ru}^{\text{II}}[(\text{terpy})(\text{bpy})\text{X}]]$ (X = PC linker) with different masses to various targeting moieties. In fact, it is possible to diversify the Ru mass-tags varying the terpy and bpy scaffolds (e.g. adding a substituent on their aromatic rings) in order to have photocleaved

fragments of different mass for every applied targeted mass-tag. Each of the latter can be linked to a different targeting epitope corresponding to different proteins of interest.

Further work is necessary to characterize the properties of compound **3** $[\text{Ru}^{\text{II}}(\text{terpy})(\text{bpy})(\text{D-biotin})(\text{cyc}(\text{RGDFK}))]^{2+}$ as photocleavable mass-tag in LDI-MSI, such as its specificity in different tissue samples and photocleavage yield. For its potential application in multiplexed analysis of proteins in a single measurement, Ru-based mass-tags have to be designed with differently modified polypyridine ligands, featuring different masses and bioconjugable to various targeting moieties.

Typically, the wavelengths of UV lasers used in MALDI-MS instruments are 337 nm (nitrogen lasers), 355 nm or 266 nm (frequency-tripled and quadrupled Nd:YAG lasers, respectively). However, the judicious modification of the Ru(II) mass-tag scaffold allows to induce photocleavage at different wavelengths.^{40–42} For example, infra-red (IR) wavelengths may be used, which may also allow deeper penetration of the photons in living tissues. Moreover, the MSI spatial resolution can be further improved, for example by using displacement of the laser in smaller steps than the N₂ laser beam diameter (5–50 μm), using a laser beam of smaller diameter⁴³ or applying transmission geometry.⁴⁴ In summary, we present here a new photochemical tool for sensitive matrix-free targeted LDI-MSI of proteins that may have far-reaching applications.

The University of Groningen is acknowledged for funding. J. H. thanks the China Scholarship Council (CSC) for a PhD fellowship.

Conflicts of interest

There are no conflicts to declare.

References

- 1 P. Mallick and B. Kuster, *Nat. Biotechnol.*, 2010, **28**, 695–709.
- 2 Y.-J. Xue, H. Gao, Q. C. Ji, Z. Lam, X. Fang, Z. Lin, M. Hoffman, D. Schulz Jander and N. Weng, *Bioanalysis*, 2012, **4**, 2637–2653.
- 3 C. G. Hartinger, M. Groessl, S. M. Meier, A. Casini and P. J. Dyson, *Chem. Soc. Rev.*, 2013, **42**, 6186–6199.
- 4 M. Wenzel and A. Casini, *Coord. Chem. Rev.*, 2017, **352**, 432–460.
- 5 R. M. Caprioli, T. B. Farmer and J. Gile, *Anal. Chem.*, 1997, **69**, 4751–4760.
- 6 R. D. Addie, B. Balluff, J. V. M. G. Bovée, H. Morreau and L. A. McDonnell, *Anal. Chem.*, 2015, **87**, 6426–6433.
- 7 P. M. Vaysse, R. M. A. Heeren, T. Porta and B. Balluff, *Analyst*, 2017, **142**, 2690–2712.
- 8 J. Han, H. Permentier, R. Bischoff, G. Groothuis, A. Casini and P. Horvatovich, *TrAC, Trends Anal. Chem.*, 2019, **112**, 13–28.
- 9 A. Walch, S. Rauser, S.-O. Deininger and H. Höfler, *Histochem. Cell Biol.*, 2008, **130**, 421–434.
- 10 M. Niehaus, J. Soltwisch, M. E. Belov and K. Dreisewerd, *Nat. Methods*, 2019, **16**, 925–931.
- 11 F. Deutschens, J. Yang and R. M. Caprioli, *J. Mass Spectrom.*, 2011, **46**, 568–571.
- 12 P.-M. Vaysse, R. M. A. Heeren, T. Porta and B. Balluff, *Analyst*, 2017, **142**, 2690–2712.
- 13 R. J. a. Goodwin, *J. Proteomics*, 2012, **75**, 4893–4911.
- 14 G. Thiery, M. S. Shchepinov, E. M. Southern, A. Audebourg, V. Audard, B. Terris and I. G. Gut, *Rapid Commun. Mass Spectrom.*, 2007, **21**, 823–829.
- 15 R. Lemaire, J. Stauber, M. Wisztorski, C. Van Camp, A. Desmons, M. Deschamps, G. Proess, I. Rudlof, A. S. Woods, R. Day, M. Salzet and I. Fournier, *J. Proteome Res.*, 2007, **6**, 2057–2067.
- 16 J. Olejnik, E. Krzymańska-Olejnik and K. J. Rothschild, *Methods Enzymol.*, 1998, **291**, 135–154.
- 17 J. Stauber, M. El Ayed, M. Wisztorski, R. Day, I. Fournier and M. Salzet, *Anal. Chem.*, 2009, **81**, 9512–9521.
- 18 J. Yang, P. Chaurand, J. L. Norris, N. A. Porter and R. M. Caprioli, *Anal. Chem.*, 2012, **84**, 3689–3695.
- 19 G. Thiery, R. L. Mernaugh, H. Yan, J. M. Spraggins, J. Yang, F. F. Parl and R. M. Caprioli, *J. Am. Soc. Mass Spectrom.*, 2012, **23**, 1689–1696.
- 20 G. Thiery-Lavenant, A. I. Zavalin and R. M. Caprioli, *J. Am. Soc. Mass Spectrom.*, 2013, **24**, 609–614.
- 21 D. Havrylyuk, K. Stevens, S. Parkin and E. C. Glazer, *Inorg. Chem.*, 2020, **59**, 1006–1013.
- 22 S. Campagna, F. Puntoriero, F. Nastasi, G. Bergamini and V. Balzani, *Photochemistry and Photophysics of Coordination Compounds I*, Springer, Berlin, Heidelberg, 2007, pp. 117–214.
- 23 S. Bonnet and J.-P. Collin, *Chem. Soc. Rev.*, 2008, **37**, 1207–1217.
- 24 R. Haubner, R. Gratijs, B. Diefenbach, S. L. Goodman, A. Jonczyk and H. Kessler, *J. Am. Chem. Soc.*, 1996, **118**, 7461–7472.
- 25 T. G. Kapp, F. Rechenmacher, S. Neubauer, O. V. Maltsev, E. A. Cavalcanti-Adam, R. Zarka, U. Reuning, J. Notni, H. J. Wester, C. Mas-Moruno, J. Spatz, B. Geiger and H. Kessler, *Sci. Rep.*, 2017, **7**, 1–13.
- 26 M. Nieberler, U. Reuning, F. Reichart, J. Notni, H.-J. Wester, M. Schwaiger, M. Weinmüller, A. Räder, K. Steiger and H. Kessler, *Cancers*, 2017, **9**, 116.
- 27 J. Schittenhelm, A. Klein, M. S. Tatagiba, R. Meyermann, F. Fend, S. L. Goodman and B. Sipos, *Int. J. Clin. Exp. Pathol.*, 2013, **6**, 2719–2732.
- 28 K. Hovidala-Dilke, *Curr. Opin. Cell Biol.*, 2008, **20**, 514–519.
- 29 J. S. Desgrosellier and D. A. Cheresch, *Nat. Rev. Cancer*, 2010, **10**, 9–22.
- 30 E. M. Fabricius, G. P. Wildner, U. Kruse-Boitschenko, B. Hoffmeister, S. L. Goodman and J. D. Raguse, *Exp. Ther. Med.*, 2011, **2**, 9–19.
- 31 N. Kaveevivitchai, R. Zong, H. W. Tseng, R. Chitta and R. P. Thummel, *Inorg. Chem.*, 2012, **51**, 2930–2939.
- 32 J. Rodríguez, J. Mosquera, J. R. Couceiro, M. E. Vázquez and J. L. Mascareñas, *Angew. Chem., Int. Ed.*, 2016, **55**, 15615–15618.
- 33 R. E. Goldbach, I. Rodríguez-García, J. H. Van Lenthe, M. A. Siegler and S. Bonnet, *Chem. – Eur. J.*, 2011, **17**, 9924–9929.
- 34 R. Beavis, J. Lindner, J. Grotemeyer, I. M. Atkinson, F. R. Keene and A. E. W. Knight, *J. Am. Chem. Soc.*, 1988, **110**, 7534–7535.
- 35 J. E. Ham, B. Durham and J. R. Scott, *J. Am. Soc. Mass Spectrom.*, 2003, **14**, 393–400.
- 36 R. Beavis, J. Lindner, J. Grotemeyer, I. M. Atkinson, F. R. Keene and A. E. W. Knight, *J. Am. Chem. Soc.*, 1988, **110**, 7534–7535.
- 37 X. Liang, S. Suwanrumpha and R. B. Freas, *Inorg. Chem.*, 1991, **30**, 652–658.
- 38 A. O. Frank, E. Otto, C. Mas-Moruno, H. B. Schiller, L. Marinelli, S. Cosconati, A. Bochen, D. Vossmeier, G. Zahn, R. Stragies, E. Novellino and H. Kessler, *Angew. Chem., Int. Ed.*, 2010, **49**, 9278–9281.
- 39 J. Han, A. F. B. Räder, F. Reichart, B. Aikman, M. N. Wenzel, B. Woods, M. Weinmüller, B. S. Ludwig, S. Stürup, G. M. M. Groothuis, H. P. Permentier, R. Bischoff, H. Kessler, P. Horvatovich and A. Casini, *Bioconjugate Chem.*, 2018, **29**, 3856–3865.
- 40 J. K. White, R. H. Schmehl and C. Turro, *Inorg. Chim. Acta*, 2017, **454**, 7–20.
- 41 D. Havrylyuk, K. Stevens, S. Parkin and E. C. Glazer, *Inorg. Chem.*, 2020, **59**, 1006–1013.
- 42 A. Soupart, F. Alary, J.-L. Heully, P. I. P. Elliott and I. M. Dixon, *Coord. Chem. Rev.*, 2020, **408**, 213184.
- 43 A. Zavalin, J. Yang and R. Caprioli, *J. Am. Soc. Mass Spectrom.*, 2013, **24**, 1153–1156.
- 44 A. Zavalin, J. Yang, K. Hayden, M. Vestal and R. M. Caprioli, *Anal. Bioanal. Chem.*, 2015, **407**, 2337–2342.